Identifying Technical and Economic Improvements to the MoneyMaker Hip Pump through Multi-Objective Optimization

Christopher McComb[1], Pablo S. Santaeufemia[1], Nathan G. Johnson[2], and Kenji Shimada[1]
[1] Department of Mechanical Engineering, Carnegie Mellon University, Pittsburgh, Pennsylvania, U.S.A.
[2] Department of Engineering and Computer Systems, Arizona State University, Mesa, Arizona, U.S.A.

***Abstract*—Water-lifting technologies in rural areas of the developing world have enormous potential to stimulate agricultural production and economic growth. The MoneyMaker Hip pump designed by Kickstart is a human-powered low cost pump, which can help subsistence farmers increase financial returns. This work optimizes the design of the MoneyMaker Hip pump, which is the cheapest and lightest portable water pump from Kickstart. A mathematical model of the working fluid and MoneyMaker Hip pump structure is developed. Deterministic optimization methods are then employed to maximize the flow rate of the groundwater pumped, maximize the lift height, and minimize the volume of material used for manufacturing. Design variables for the optimization included the dimensions of the pump, well depth, and speed of various parts of the system. The solutions are subject to constraints on the geometry of the system, the bending stress in the handle and cylinder, and ergonomic factors. Findings indicate that several technical improvements can be made on the current MoneyMaker Hip pump design to reduce the cost and human workload.**

Keywords—manual pump; design; multi-objective optimization; developing world.

I. Introduction

Rural villages in developing countries are typified by many hardships—lack of basic infrastructure, little or no health care facilities, limited educational opportunities, poor access to clean water and energy, and limited opportunities for jobs and economic growth. Significant financial, material, and managerial aid has been provided over the last sixty years by governmental and non-governmental organizations to address these problems, yet the extent of poverty in rural areas has remained largely unchanged [1]. More recently, market-based approaches that develop entrepreneurial activities have shown promise to reducing poverty through local business development and increased income. In noting that farming is the primary occupation in rural areas, many organizations have worked to increase crop yield through improved irrigation techniques [2]. Reliable irrigation techniques have been shown to increase crop yields between 100%-400% [3]. The resulting increase in grain volume translates to increased sales and income, and allows farmers to cultivate higher-value crops, adopt new technologies, and increase financial returns. Despite the benefits of irrigation, too few farmers have a steady source of irrigation due to the financial limitations of acquiring commercial irrigation technologies.

Diesel pumps are effective for irrigation yet the capital cost and fuel costs are too high for diesel pumps to be commonplace. Human-powered pumps—such as a treadle or hand pump—with low capital cost and minimal ongoing cost have become a popular option for farmers with small plots of land [4]. A treadle pump is operated by stepping up and down on treadles to actuate two pistons that create suction and draw groundwater to the surface. Since the first treadle pump was invented by the Norwegian engineer Gunnar Barnes in 1970, companies such as International Development Enterprises (IDE), Kickstart and others have re-designed the treadle pump and offered hand pumps to serve a wider range of customers by adapting the technology to the geographic, environmental, economic and cultural requirements of customers.

Common treadle pump designs enable the pumping of water from depths of up to seven meters and allows for a flow-rate of up to five liters per second [5, 6]. Kickstart recognized that groundwater in many countries in Africa tends to be deeper than other regions and in response to farmers' demands, Kickstart modified the basic treadle design to achieve greater depth [7, 8]. The redesigned MoneyMaker pumps (Fig. 1) from Kickstart facilitated sprinkler irrigation, which replaced many of the suction-only pumps in the region, and operated as a hand pump rather than a treadle pump. Such design changes have enabled Kickstart to expand their human powered pump sales in many different countries in Africa.

Fig. 1. The MoneyMaker Hip Pump

Additional research is needed to reduce cost, increase performance, and facilitate mass manufacturing of treadle pumps [9, 10]. Work by Wood & Lewis led to the creation of a modular treadle pump design that could be reconfigured with additional components to achieve increasingly higher performance pumps [9], this innovative technical approach was rooted in an appreciation for local economic constraints in that early modules could be purchased at a low cost and the resulting earnings could be used to purchase more expensive yet high-performing modules. More recently, multi-objective optimization techniques have been applied in work by Santaeufemia et al. to maximize water output while reducing cost [10]. The work presented herein applies similar optimization techniques to the MoneyMaker Hip Pump to improve the operating characteristics (flow and water tank height) of a pump while minimizing cost. Additionally, a computational fluid dynamics (CFD) model has been developed using computer aided drafting (CAD) models to validate optimization results. A range of design options is analyzed in pursuit of a cheaper pump with greater marketability for low-income farmers.

II. The Physical System

Fig. 2 shows the MoneyMaker Hip Pump with relevant variables labeled. The inner and outer diameters of the pump inlet hose are denoted by x_1 and x_2 while x_9 and x_{10} are the inner and outer diameters of the outlet hose. The inner and outer diameters of the pump cylinder are denoted by x_3 and x_4, respectively, and x_5 is the length of the pump cylinder, which is directly related to the pump stroke length. The variables x_6, x_7, x_{11} and x_{12} describe the positive of the pump relative to the water source and the tank. The operation of the pump is described by x_{13} and x_{14} (the forces for the downstroke and upstroke) and x_{15} and x_{16} (the velocities of the downstroke and upstroke).

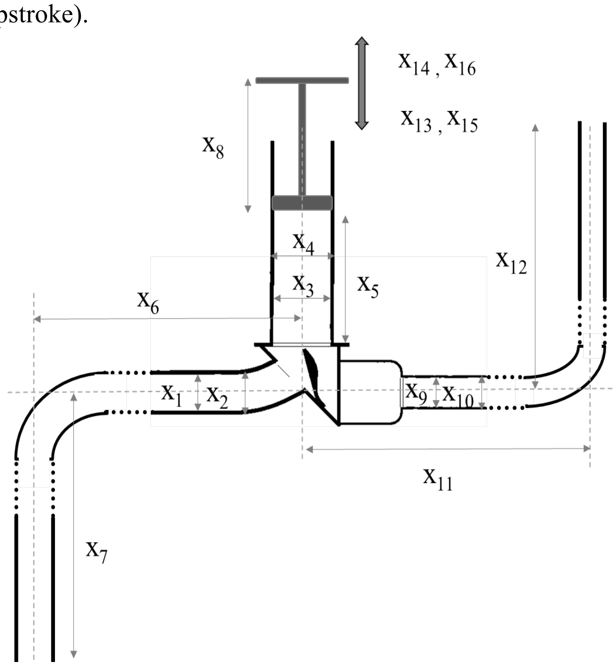

Fig. 2. Design dimensions, forces, and velocities of the MoneyMaker Hip Pump.

III. Methodology

The first half of the analysis was carried out using multi-objective optimization to examine the effect of design dimensions on conflicting objective functions including flow rate, height of the pumped water column, and pump cost. The second half of the analysis validated the optimization results using CFD models that describe the physical and fluidic operation of the manual pump.

A. Multi-objective Optimization

An optimization study was undertaken to maximize the flow rate of the pump and maximize the height to which water could be pumped while simultaneously minimizing the cost of the pump. The first two objectives, flow rate (F_1) and height (F_2), are easily computed as:

$$F_1(x) = (0.25\pi x_3{}^2 x_5)\left(\frac{x_5}{x_{15}}+\frac{x_5}{x_{16}}\right)^{-1} \tag{1}$$

$$F_2(x) = x_{12} \tag{2}$$

The third objective, cost (F_3), was calculated using a more complicated function that accounts for the volume of material, cost of material, and cost of connections between different pump sections:

$$F_3(x)= C_{h,in}+C_{h,out}+C_{cyl}+C_{pist}+C_{body} \tag{3}$$

$$C_{h,in}=C_{HDPE}0.25\pi(x_6+x_7)(x_2{}^2-x_1{}^2) \tag{4}$$

$$C_{h,out}=C_{HDPE}0.25\pi(x_{11}+x_{12})(x_{10}{}^2-x_9{}^2) \tag{5}$$

$$C_{cyl}=C_U\left(\frac{x_4}{x_{4,R}}\right) + C_{PC}\left(\frac{x_4-x_3}{x_{4,R}-x_{3,R}}\right)\left(\frac{x_5}{x_{5,R}}\right) \tag{6}$$

$$C_{pist}=C_{SW}\left(\frac{x_3-0.006}{x_{3,R}-0.006}\right)^2 +C_{LW}\left(\frac{x_3}{x_{3,R}}\right)^2 \dots + C_{HR}\left(\frac{x_8}{x_{8,R}}\right)+C_{SC}\left(\frac{x_4}{x_{4,R}}\right) \tag{7}$$

$$C_{body}=C_{IPL}\left(\frac{x_1}{x_{1,R}}\right)^2 +C_{OPL}\left(\frac{x_9}{x_{9,R}}\right)^2 \dots +C_{TPL}\left(\frac{x_3}{x_{3,R}}\right)^2 +C_N\left(\frac{x_3}{x_{3,R}}\right) \dots +C_{OP}\left(\frac{x_9}{x_{9,R}}\right)+C_{IP}\left(\frac{x_1}{x_{1,R}}\right) \tag{8}$$

This function references costs of many components to those in Kickstart's current design, scaling them accordingly. While the list of parts is not exhaustive, it contains the largest and most expensive components. The cost of hoses was calculated according to material volume assuming a constant volumetric cost provided by Kickstart.

TABLE I. CONSTANT VALUES FOR OBJECTIVE FUNCTION

Constant	Description	Value
C_U	Cost of union between cylinder and valve box	0.75 USD
C_{PC}	Cost of pump cylinder	1.96 USD
C_{SW}	Cost of small washer	0.31 USD
C_{LW}	Cost of large washer	0.45 USD
C_{HR}	Cost of handle rod	1.57 USD
C_{SC}	Cost of splash cup	0.74 USD
C_{IPL}	Cost of inlet plate	0.88 USD
C_{OPL}	Cost of outlet plate	1.09 USD
C_{TPL}	Cost of top plate	1.09 USD
C_N	Cost of nipple	1.05 USD
C_{OP}	Cost of outlet pipe	1.13 USD
C_{IP}	Cost of inlet pipe	1.07 USD
C_{HDPE}	Volumetric cost of HDPE	3808 USD/m^3
$x_{1,R}$	Reference value of x1	0.017 m
$x_{3,R}$	Reference value of x3	0.045 m
$x_{4,R}$	Reference values of x4	0.05 m
$x_{5,R}$	Reference value of x5	0.632 m
$x_{8,R}$	Reference value of x8	0.687 m
$x_{9,R}$	Reference value of x9	0.019 m

Optimization was performed with respect to several constraints. Equality constraints are provided in Table II and inequality constrains are provided in Table III. The function H_L is defined to allow equality constraints to be more succinctly described in calculating the major loss in the pipe

$$H_L(L,V,D)=\frac{10.67L\left(0.25\pi D^2V\right)^{1.85}}{{C_{HW}}^{1.85}D^{4.87}} \tag{9}$$

where L is the length of the pipe, D is its diameter, and V is the velocity of the fluid. Further, the function H_P is defined to calculate the head added by a pumping action

$$H_P(F,D)=\frac{F}{\rho g 0.25\pi D^2} \tag{10}$$

where F is the force of the pumping action, and D is the diameter of the pipe.

TABLE II. EQUALITY CONSTRAINTS USED IN OPTIMIZATION MODEL

Equation	Description
$h_1(x)=x_2-1.0945x_1-\frac{2.841}{1000}$	Relationship between inner and outer diameter of inlet hose
$h_2(x)=x_4-1.0945x_3-\frac{2.841}{1000}$	Relationship between inner and outer diameter of pump cylinder
$h_3(x)=x_{10}-1.0945x_9-\frac{2.841}{1000}$	Relationship between inner and outer diameter of outlet hose
$h_4(x)=H_L(x_6+x_7,x_{16},x_1)+H_L(0.5x_5,x_{16},x_3)\ldots$ $+x_7+0.5x_5+\frac{{x_{16}}^2}{2g}-H_P(x_{14},x_3)$	Constraint to solve fluid equation during upstroke
$h_5(x)=H_L(x_{11}+x_{12},x_{15},x_9)+H_L(0.5x_5,x_{15},x_3)\ldots$ $+x_7-0.5x_5-\frac{{x_{15}}^2}{2g}-H_P(x_{13},x_3)$	Constraint to solve fluid equation during downstroke
$h_6(x)=x_7-d_{well}$	Depth of well
$h_7(x)=x_6+x_{11}-d_{horiz}$	Constraint on horizontal distance from tank to well

The equations for h_1, h_2 and h_3 were developed by performing a regression analysis on a set of pipe diameter data. The data, and the resulting linear fit, are shown in Fig. 3.

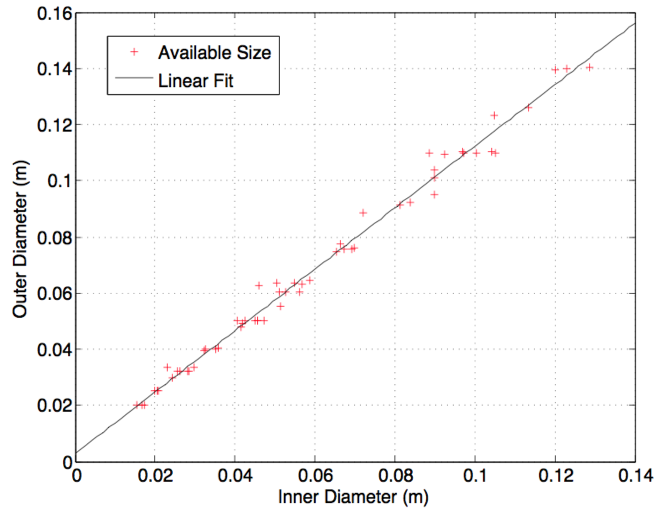

Fig. 3. Regression analysis for available hose sizes.

Inequality constraints were also implemented in the model. These modeled a variety of physical phenomena and human factors provided in Table III. Constraints g_1 and g_2 limit the power that can be applied to the handle by the human operator. These limits on power input were calculated from experimental data provided by Kickstart (specifically, force applied to the handles and average velocity of the piston). The resultant limiting power values are provided in Table IV alongside other parameters and constraints.

TABLE III. INEQUALITY CONSTRAINTS USED IN OPTIMIZATION MODEL

Equation	Description
$g_1(x)=x_{13}x_{15}-P_{down}$	Upper limit on average downstroke power
$g_2(x)=x_{14}x_{16}-P_{up}$	Upper limit on average upstroke power
$g_3(x)=x_5+x_8-d_{shoulder}$	Upper limit on top extent of stroke
$g_4(x)=d_{knee}-x_8$	Lower limit on bottom extent of stroke
$g_5(x)=t_{cycle}-\left(\frac{x_5}{x_{15}}+\frac{x_5}{x_{16}}\right)$	Minimum cycle time
$g_6(x)=x_5\text{-}x_8$	Piston much be longer than cylinder
$g_7(x)=\frac{x_{14}}{0.25\pi {x_3}^2}-p_{vp}$	Protects against cavitation during upstroke

Since this problem is described using three objective functions, the solution is a Pareto front rather than a single pump design. To resolve the Pareto front, a series of cases were optimized by specifying values for F_1 and F_2 (through additional equality constraints), and then minimizing F_3. Each case was solved using the `fmincon` function in MATLAB. The sequential quadratic programming (SQP) algorithm was used with merit-function line search and quasi-Newton Hessian updating. This algorithm was chosen because many of the functions in this problem are quadratic. Additionally, the SQP algorithm is robust to undefined function evaluations, which aided convergence in our problem. The algorithm was terminated when first order optimality was satisfied to within 10^{-6} and the maximum constraint violation was 10^{-6}. This process was completed several times with starting points randomized for each case to increase the likelihood that global optima were found.

TABLE IV. PARAMETERS AND CONSTANTS

Constant	Description	Value
P_{down}	Average power supplied during downstroke	27.7 W
P_{up}	Average power supplied during upstroke	33.7 W
$d_{shoulder}$	Average height of shoulder	1.3 m
d_{knee}	Average height of knee	0.5 m
t_{cycle}	Upper limit on cycle time	3 s
g	Gravitational constant	9.8 m/s^2
C_{HW}	Hazen-Williams coefficient for water	140
ρ	Density of water	1000 kg/m^3
d_{well}	Depth of well	7 m
d_{horiz}	Distance from well to tank	18 m
p_{vp}	Vapor pressure of water	101.3 kPa

B. Computational Fluid Analysis

The flow in the Kickstart Hip Pump was simulated using Autodesk Simulation CFD 2014 software. The current CAD model was provided by the company (Fig. 4) and then simplified using Autodesk Inventor 2014 (Fig. 5).

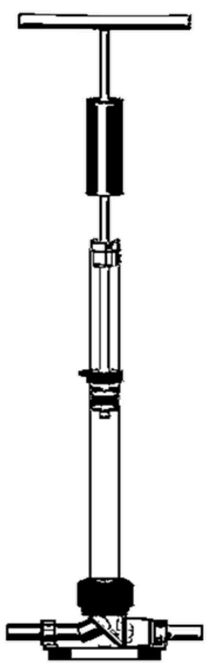

Fig. 4. CAD Model for Kickstart's MoneyMaker Hip Pump

The pump was modeled with a valve opening of 35 degrees at the suction and pressure sides of the valve box. This number was defined using the experimental data provided by Kickstart. Moreover, based on Kickstart's customers current use the pump had attached an inlet and an outlet hose of 20.6mm ID and 25.12mm OD respectively. The horizontal distance from the water source to a water tank was standardized to be 18 meters and the standard height of location for their water tank was 3 meters high.

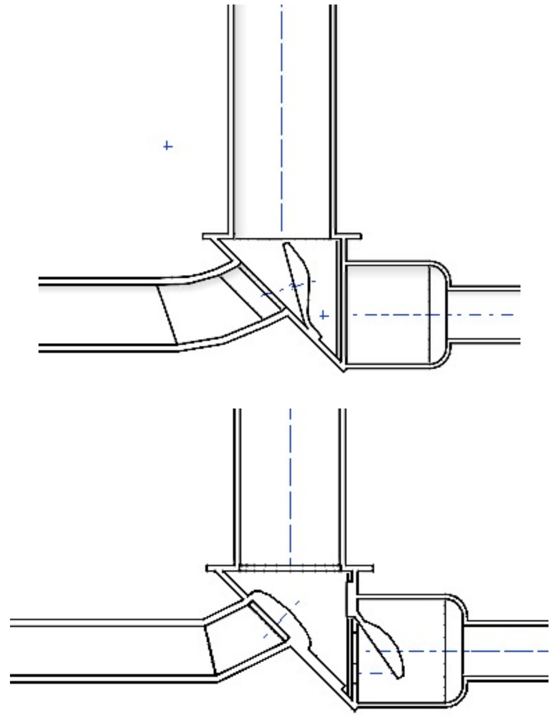

Fig. 5. Simplified CAD Model for suction (top) and pressure (bottom).

The objective of the CFD simulation is to validate the results of the optimization model. Hence, separate models were produced for the upstroke and the downstroke. The upstroke has the suction valve 35 degrees opened and the pressure valve is fully close, while the downstroke model has the pressure valve 35 degrees opened and the suction valve is fully closed. Two pressure boundary conditions were set in each model. On the suction side, the inlet pressure is atmospheric pressure while the outlet pressure is the vacuum pressure created by the piston on the upstroke. On the pressure side, the inlet pressure is the pressure created by the piston on the downstroke while the outlet pressure is atmospheric pressure. Each CFD model contained approximately 350,000 elements. The solution was set to run for 200 steps to allow for convergence.

IV. RESULTS

A. Multi-objective Optimization

Multiple combinations of tank height and flow rate were explored for the optimization study. Tank height was varied from 0 m to 3 m, in increments of 1 m. The flow rate was varied from 0.00 l/s to 0.40 l/s in increments of 0.02 l/s. The optimization described above was completed for each combination of values. The Pareto front resulting from this procedure is provided in Fig. 6.

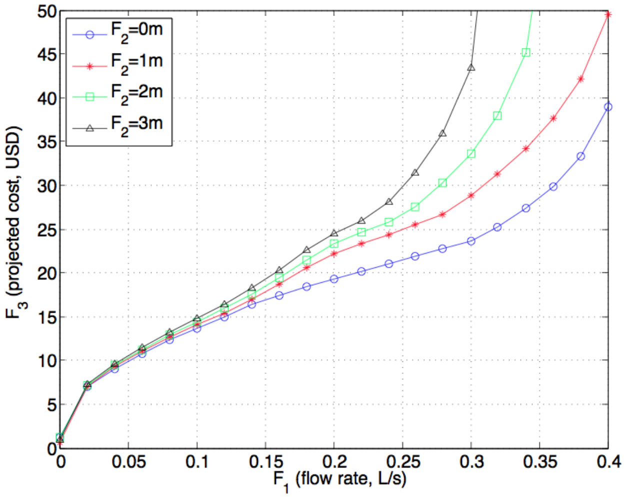

Fig. 6. Pareto front resulting from optimization study

Several representative designs corresponding to a range of operating conditions are provided in Table V. These can be compared to the dimensions and operating conditions of the Kickstart Moneymaker pump. Note that the flow rate for the Moneymaker pump is a value provided by Kickstart. Corresponding diagrams for the designs in the table are provided in Fig. 7.

TABLE V. REPRESENTATIVE OPTIMAL DESIGNS

	Moneymaker	**Low Flow No Tank**	**High Flow No Tank**	**Low Flow Tall Tank**	**High Flow Tall Tank**
F1	0.25 l/s	0.14 l/s	0.3 l/s	0.14 l/s	0.3 l/s
F2	3 m	0 m	0 m	3 m	3 m
F3	31.48 USD	16.41 USD	23.61 USD	18.23 USD	43.37 USD
x1	0.0220 m	0.0140 m	0.0180 m	0.0140 m	0.0274 m
x2	0.0210 m	0.0182 m	0.0225 m	0.0182 m	0.0328 m
x3	0.0450 m	0.0355 m	0.0434 m	0.0355 m	0.0433 m
x4	0.0500 m	0.0417 m	0.0504 m	0.0417 m	0.0502 m
x5	0.6320 m	0.5000 m	0.6829 m	0.5000 m	0.06875 m
x6	3.0000 m	0.0000 m	18.0000 m	0.0000 m	18.0000 m
x7	7.0000 m	7.0000 m	7.0000 m	7.0000 m	7.0000 m
x8	0.687 m	0.5000 m	0.6830 m	0.5000 m	0.6875 m
x9	0.0220 m	0.0115 m	0.0012 m	0.0126 m	0.0327 m
x10	0.0190 m	0.0154 m	0.0041 m	0.0166 m	0.0386 m
x11	15.0000 m	18.0000 m	0.0000 m	18.0000 m	0.0000 m
x12	3.0000 m	0.0000 m	0.0000 m	3.0000 m	3.0000 m
x13	159.9 N	113.1 N	6.9 N	113.1 N	40.9 m
x14	161.9 N	100.1 N	150.0 N	100.1 N	115.1 m
x15	0.2106 m/s	0.2449 m/s	4.0000 m/s	0.2449 m/s	0.6774 m/s
x16	0.1755 m/s	0.3361 m/s	0.2135 m/s	0.3361 m/s	0.2922 m/s

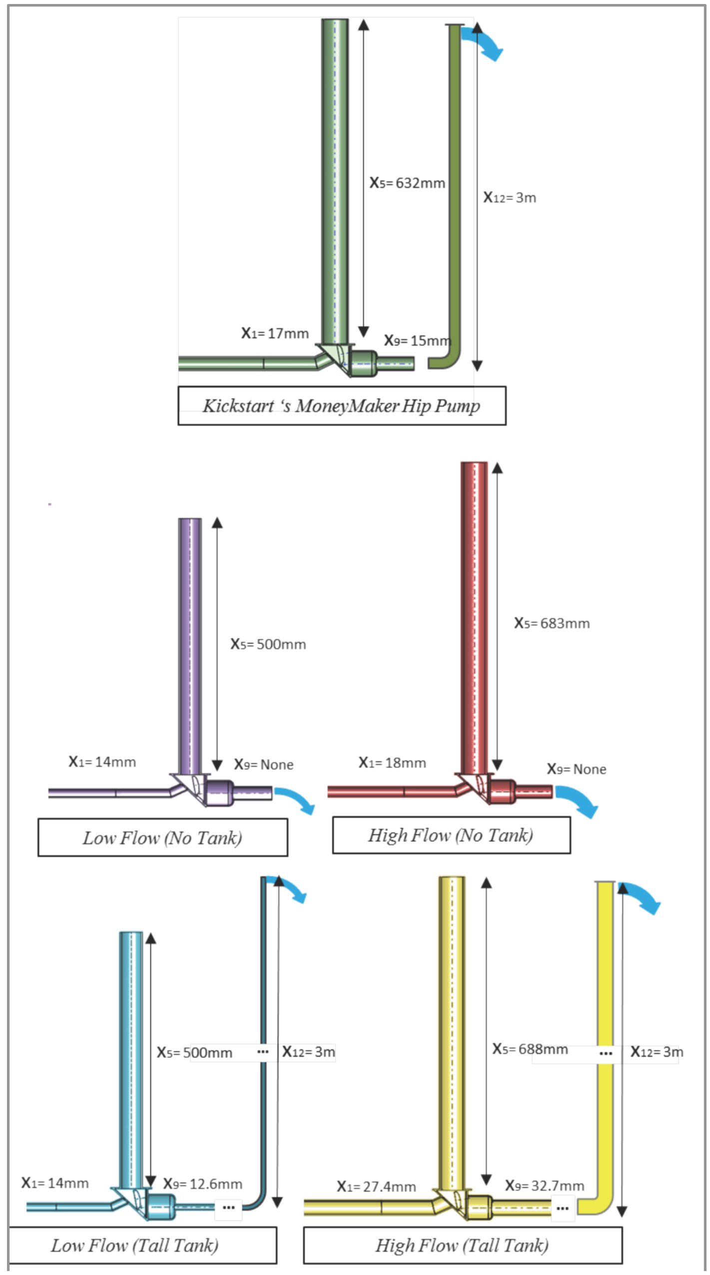

Fig. 7. CAD Models for representative optimal designs.

Both no-tank and tall tank solutions are very similar for the low flow-rate case, but are significantly different for the high flow-rate case. To further illustrate the difference between designs, Fig. 8 shows the 2-norm of the partial solution vector [x_1, x_2, x_3, x_4, x_5, x_8, x_9, x_{10}] for each Pareto solution. From Fig. 8, it becomes apparent that solutions are independent of tank height up to a flow rate of 0.14 L/s. Past this, solutions for cases with non-zero tank heights are simply a function of flow rate up to 0.22 L/s. Above 0.22 L/s, the difference between solutions increases markedly.

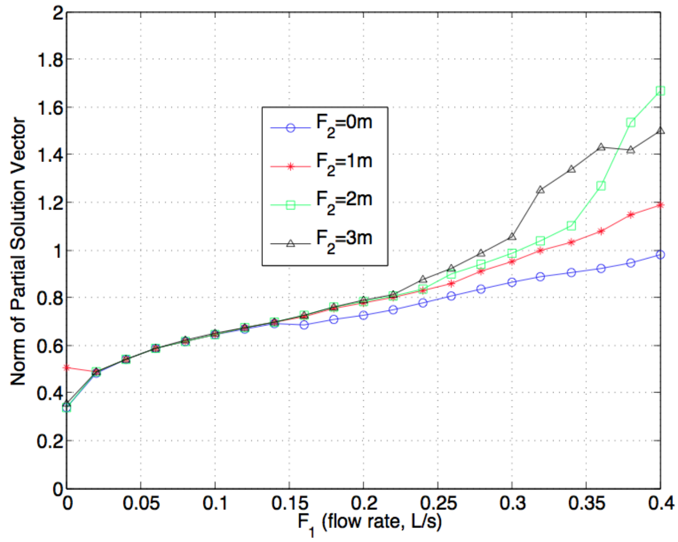

Fig. 8. Norm of partial solution vector, indicating similarity of designs.

Another trend made apparent in Table V is the dichotomous nature of the placement of the pump (x_6 and x_{11}). It is clearly better to place the pump over the well for low flow rate use cases, which is converse to high flow rate use cases in which it is better to place the pump at the tank location. This tradeoff occurs at a flow rate of approximately 0.18 l/s. To further understand these representative designs an examination follows of Lagrange multipliers associated with each constraint. These are provided in Table VI.

TABLE VI. LAGRANGE MULTIPLIER VALUES FOR REPRESENTATIVE OPTIMAL DESIGNS

Constraint	Low Flow No Tank	High Flow No Tank	Low Flow Tall Tank	High Flow Tall Tank
h_1	76.1	336.4	76.1	-490.8
h_2	34.0	45.34	34.0	-45.6
h_3	165.6	0.0	208.3	-69.3
h_4	-31893.4	-135051.8	-31893.4	1169240.8
h_5	-13491.4	-937.4	-23497.4	1506211.8
h_6	5.4	1391382.7	5.4	-171.5
h_7	4.0	1391382.6	4.0	-13.0
g_1	56.9	0.2	99.1	1544.1
g_2	43.6	0.0	88.3	2778.4
g_3	0.0	0.0	0.0	0.7
g_4	0.5	0.0	0.5	0.0
g_5	0.8	1.5	0.8	1.3
g_6	1.8	2.3	1.8	2.9
g_7	0.0	0.0	0.0	0.0

Examining the relative magnitude of the Lagrange multipliers associated with a given solution can indicate the relative importance of the associated constraint. By examining the equality constraints, it becomes apparent that the constraints on the fluid solution (h_4 and h_5) generally have the largest Lagrange multipliers. The large Lagrange multipliers associated with h_6 and h_7 for the high flow tankless scenario are an artifact that occurs for cases when the pump is placed at the tank location, and high flow is required.

Examining the inequality constraints yields additional insight into the solutions. For an inequality constraint, a Lagrange multiplier of 0 indicates that the associated constraint is inactive, meaning that it does not influence the optimal solution. For the solutions shown, g_7 never has a meaningfully large Lagrange multiplier, meaning that it does not influence the solution substantially. Constraints on the extent of the stroke (g_3 and g_4) also tend to have little impact on the solution. The most important are generally the constraints on power, g_1 and g_2.

B. Computational Fluid Analysis

The suction and pressure CFD solutions in Autodesk Simulation CFD converged at the 168th and 182nd step respectively. In Fig. 9, the velocity magnitude profiles are shown for the suction (left) and pressure (right) CFD simulations. As seen in Table VII, the velocity along the cylinder is higher when pushing than when pulling the pump handle. The total cycle time was calculated to be 4.59 seconds, with a corresponding average flow rate of 0.219 l/s.

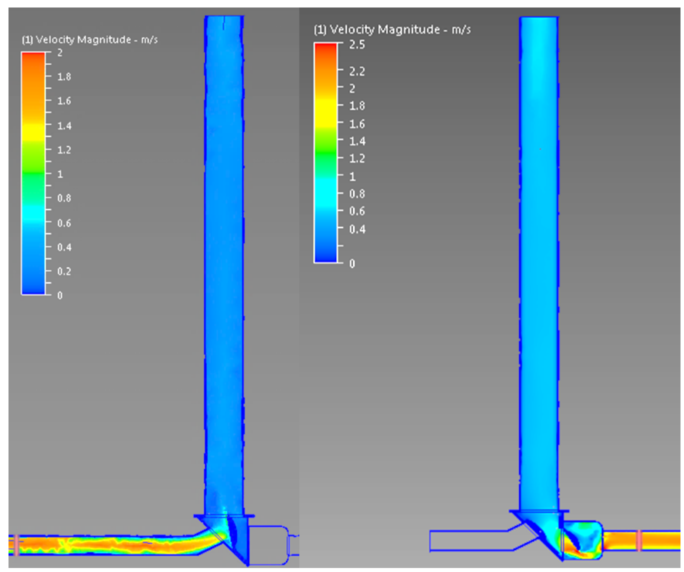

Fig. 9. Suction (left) and Pressure (right) CFD Solution (200th Step).

TABLE VII. CFD RESULTS FOR SUCTION & PRESSURE MODELS

Parameter	Suction	Pressure
Flow velocity along pump cylinder	0.2008 m/s	0.4385 m/s
Time required	3.15 s	1.44 s
Average Flow Rate	0. 219 L/s	
Total Cycle Time	4.59 s	

The average flow rate for the CFD simulation is 0.219 l/s. This is comparable to the value of 0.25 l/s experimentally measured by Kickstart According to their experimental data the upstroke and downstroke take 3.6 and 3.0 seconds, respectively. The greatest disparity in the results with the optimization models originates in the velocity of the pressure side model. This is likely caused by the assumption that the flow on the pressure side is laminar and there are no disturbances.

V. CONCLUSION

This work presented a methodology for optimizing the physical construction of a hand-operated water pump. First, the physical system was examined. Second, an approriate simplied optimization model was developed. This model considered a variety of constraints to ensure the validity of the model, and also defined three important objectives. Third, an optimization study was performed with this model, and optimal designs were compared. Fourth, CFD was utilized to gain greater insight to the operation of the optimal designs.

The results from this work indicate that there is room to improve the performance of the MoneyMaker Hip Pump. Some gains can be realized from in the placement of the pump relative to the well—the pump should be placed near the well for low flow rates and further away for large flow rates. In addition, at low flow rates the optimal solution is independent of tank height, but optimal solutions become dependent on tank height for large flow rates. Kickstart could utilize this information to develop a wider range of product options.

Future work will incorporate product modularity concepts to explore the development of several distinct pumps as a line of products with interchangeable components. In addition, it should be noted that this work focuses on the fluid operation of the pump, without modeling fatigue or mechanical failure modes. Therefore, further optimization of the valve box components will be performed using a combination of CFD and finite element analysis tools. Finally, exploring alternative materials as a means of further decreasing cost could yield substantial benefit.

ACKNOWLEDGMENT

The authors would like to thank Kickstart for their assistance with this project. The guidance of Alan Spybey (Director, Product Intelligence and Development) and Simon M. Mugo (Mechanical Engineering Designer) were particularly invaluable.

This material is based upon work supported by the National Science Foundation Graduate Research Fellowship under Grant No. DGE125252.

REFERENCES

[1] P. Polak and M. Warwick, The Business Solution to Poverty: Designing Products and Services for Three Billion New Customers. San Francisco, CA: Berrett-Koehler, 2013.

[2] J. Magistro, M. Roberts, S. Haggblade, F. Kramer, P. Polak, E. Weight, and R. Yoder, "A model for pro-poor wealth creation through small-plot irrigation and integrated service provision," in IDE International for presentation at IWMI regional workshop and policy roundtable Pro-Poor Intervention Strategies in Irrigated Agriculture in Asia, pp. 25-27, August 2004.

[3] Food and Agriculture Organization, "Water and food security," Rome, Italy: Food and Agriculture Organization, 2000, pp. 1–2.

[4] IDE–Nepal, "Natural Resource Management Approaches and Technologies in Nepal: Technology–Treadle pump," accessed online at http://lib.icimod.org/record/28280/files/Technology%20(8).pdf, January 2014.

[5] C. Bielenberg and H. Allen, How to Make and Use the Treadle Irrigation Pump, London, UK: ITDG Publishing, 1995.

[6] G. B. A. Orr and A. S. M. Nazrul Islam, The Treadle Pump Manual Irrigation for Small Farmers in Bangladesh, Dhaka, Bangladesh: Rangpur Dinajpur Rural Service, 1991.

[7] S. Hiller, "The treadle pump in Zambia: stepping out of subsistence farming," Wageningen University, 2007.

[8] I. V. Sijali and M. G. Mwago, "MoneyMaker Pumps: Creating Wealth in Sub-Saharan Africa," in Yes Africa Can: Success Stories from a Dynamic Continent, P. Chuhan-Pole and M. Angwafo, Eds., Washington, D.C.: The World Bank, 2011, pp 319-336.

[9] C. D. Wood and P. K. Lewis, "Modular Product Optimization to Alleviate Poverty: an Irrigation Pump Case Study," ASME 2012 International Design Engineering Technical Conferences & Computers and Information in Engineering Conference, 2012.

[10] P. S. Santaeufemia, N. G. Johnson, C. McComb, and K. Shimada, "Improving Irrigation in Remove Areas: Multi-objective Optimization of a Treadle Pump," ASME 2012 International Design Engineering Technical Conferences & Computers and Information in Engineering Conference, 2014.